Liquid Crystals
Publication details, including instructions for authors and subscription information:
http://www.informaworld.com/smpp/title~content=t713926090

Confinement effect on phase transitions of a discotic liquid crystal: a calorimetric study

Laurence Corvazier; Yue Zhao

Online publication date: 06 August 2010

To cite this Article Corvazier, Laurence and Zhao, Yue(2000) 'Confinement effect on phase transitions of a discotic liquid crystal: a calorimetric study', Liquid Crystals, 27: 1, 137 — 143
To link to this Article: DOI: 10.1080/026782900203317
URL: http://dx.doi.org/10.1080/026782900203317

LIQUID CRYSTALS, 2000, VOL. 27, NO. 1, 137–143

Confinement effect on phase transitions of a discotic liquid crystal: a calorimetric study

LAURENCE CORVAZIER and YUE ZHAO*

Département de chimie, Université de Sherbrooke, Sherbrooke, Québec, Canada J1K 2R1

(*Received 1 June 1999; accepted 11 August 1999*)

Differential scanning calorimetry was used to investigate the confinement effects on the phase transition behaviour of a discotic liquid crystal. The liquid crystal studied is the hexa-*n*-octanoate of rufigallol (RHO); Millipore membranes of various pore sizes were the confining materials. The polymorphism of RHO is affected by confinement. The transition from an enantiotropic columnar phase (D1) to a monotropic columnar phase (D2) is supressed in membranes with pore sizes $\leqslant 500$ Å. The transformation from D1 to the crystalline phase is also perturbed, particularly in the membrane having an average pore size of 250 Å. In the first case the crystal formed displays a double-melting endotherm, with a distinct structure melting at lower temperatures; in the other, the induction period of isothermal crystallization becomes longer and the global rate of crystallization is slowed. However, confinement shows no effect on the overall crystallization mechanism; a similar Avrami constant of $n \sim 3$ was obtained for both confined and bulk RHO. An analysis of the results is presented.

1. Introduction

Liquid crystals (LCs) are soft materials. When confined in porous media, their weak orientational and translational order can be greatly affected by contact surfaces. Generally, random surfaces in confining materials exert a dual effect of (1) aligning liquid crystals through surface anchoring, and (2) imposing disordering through the core of pores, resulting in changes in the phase transition behaviour of the LCs. Extensive studies have been dedicated to nematic and smectic liquid crystals confined in randomly distributed pores or cylinders. These studies have been reviewed in a recently published book [1]. The techniques of study employed include calorimetry [2], light scattering [3], X-ray scattering [4], dielectric spectroscopy [5], and nuclear magnetic resonance [6, 7].

Discotic liquid crystals having columnar mesophases were discovered relatively later [8] than other types of LCs. Comparatively fewer studies have been performed on this particular type of liquid crystalline material. Regarding confinement studies, to the best of our knowledge, no investigations on discotic liquid crystals have been reported so far. In this paper, we present a differential scanning calorimetric (DSC) study carried out on a discotic liquid crystal: the hexa-*n*-octanoate of rufigallol (RHO), whose chemical structure is shown below.

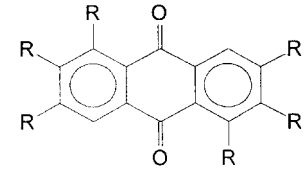

R = –O–CO–$(CH_2)_6$–CH_3

RHO is interesting because of its rich polymorphism [9, 10]. It has two columnar mesophases: an enantiotropic phase at high temperature, denoted as D1, and a monotropic phase at lower temperature, denoted as D2. As sketched in figure 1, both phases have a two-dimensional rectangular lattice, but the two lattices have different sizes and molecular orientations in the columns. In previous work [11], the unique polymorphism of RHO was explored through DSC studies of its crystallization from both columnar phases. This is another reason why RHO was chosen for the present study, since confinement effects on its phase transitions can readily be revealed by comparison with bulk RHO.

* Author for correspondence; e-mail: yzhao@courrier.usherb.ca

Liquid Crystals ISSN 0267-8292 print/ISSN 1366-5855 online © 2000 Taylor & Francis Ltd
http://www.tandf.co.uk/journals/tf/02678292.html

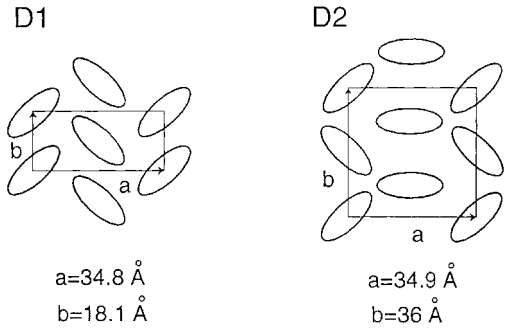

Figure 1. Schematic representation of the two-dimensional rectangular lattices of the columnar D1 and D2 phases of RHO, viewed from the columnar direction (reproduced from [10]).

2. Experimental

2.1. *Confining media*

Millipore filter papers were chosen as the confining material in this work. This type of membrane has been used in reported studies on nematic and smectic liquid crystals [2, 6, 7]. Made from pure and biologically inert mixtures of cellulose esters (nitrate and acetate), they are known to contain randomly interconnected fibrous pores, with a broad pore size distribution. Also, because of their isotropic nature, no preferential orientation of liquid crystals should be expected to arise from surface alignment [2]. As summarized in the table, three membranes of average pore sizes between 250 and 2200 Å were used to prepare confined RHO. For each membrane, the density was estimated by precisely weighing samples of known volume (over ten samples were used to obtain the mean value). Then from the density, data of pore diameter and membrane porosity, supplied by Millipore Corporation (Bedford, MA), were used to estimate the specific volume of pores and specific surface area. With a similar porosity, the specific surface area increases as the pore diameter decreases. The membrane M-250 has a specific surface area almost six times larger than the membrane M-2200.

2.2. *Preparation of confined RHO samples*

The sample of RHO used in this study was synthesized by following the method reported in [9]. The insertion of RHO into the membrane pores was made in the following way. An excess of RHO was put onto the surface of a piece of membrane, and the whole was heated to 140°C. At this high temperature, RHO was in its liquid phase, and a much reduced viscosity allowed RHO molecules to penetrate into the membrane and fill the voids progressively. Typically, after 90 min annealing, the sample was cooled to room temperature, and RHO remaining on the surface of the membrane carefully removed. Under these conditions, no significant increase was found in the amount of inserted RHO with longer annealing times. The RHO-containing membrane was then cut into small pieces and placed into a DSC pan. It was found that RHO failed to penetrate effectively into the membrane when it was in the columnar phases, probably because of reduced fluidity. In the confined RHO samples that were used for DSC measurements, the actual amount of RHO was around 7 mg. Whether the filling process was carried out inside a vacuum oven or under normal pressure made no difference to the results.

2.3. *Calorimetric measurements*

Details of the use of a Perkin-Elmer DSC-7 apparatus to determine phase transition temperatures and enthalpies of RHO were reported previously [11]. For isothermal crystallization, the crystallization rate was monitored by measuring the increase in the crystal melting endotherm with time. Typical experimental conditions were as follows: the sample was first annealed in the liquid state (140°C) for equilibrium, and was then cooled rapidly (~ 60°C min^{-1}) to a pre-selected temperature and held at this temperature for crystallization. After the desired crystallization time, a heating DSC scan was recorded. The amount of the crystal formed during that particular period of time was indicated by its heat of fusion. For the measurement of isothermal crystallization, the heating rate had little effect on the phase transition temperatures and enthalpies. For the data reported in this paper, unless otherwise stated, both heating and cooling scans were performed at a rate of 10°C min^{-1}.

3. Results

Figure 2 compares the cooling curves and subsequent heating curves of RHO confined in the membranes and non-confined RHO in the bulk, referred to hereafter as pure RHO. Pure RHO used as the reference, when cooled

Table. Characteristics of the Millipore membranes used.

Membrane	Pore diameter[a]/Å	Porosity[a]/%	Specific volume of pores/cm^3 g^{-1}	Specific surface area of pores/m^2 g^{-1}
M-250	250	70	1.23	295
M-500	500	72	1.27	152
M-2200	2200	75	1.96	53

[a] Data supplied by Millipore Corporation.

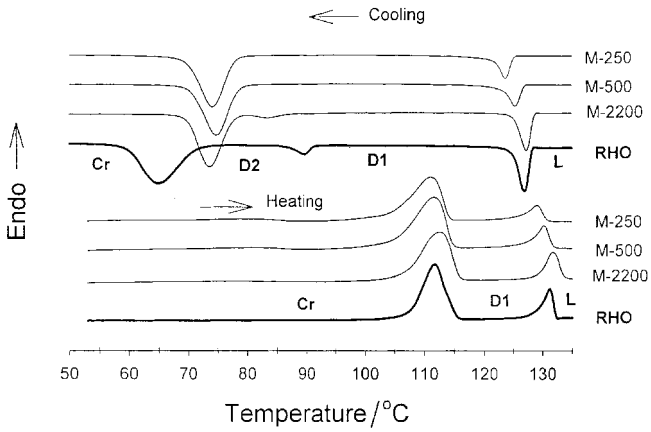

Figure 2. DSC cooling and subsequent heating curves for RHO in the bulk and RHO inserted into Millipore membranes of different pore sizes, recorded at a rate of 10°C min^{-1}.

from liquid state, shows the known phase transition sequence: liquid-to-D1 at 127°C, D1-to-D2 at 89°C and D2-to-crystal at 63°C. During the subsequent heating, the crystal melting endotherm is centred at 110°C and the D1-to-liquid transition occurs at 132°C. As compared with pure RHO, the behaviour of RHO inside the membranes indicates confinement effects on the phase transitions. The effects can be summarized as follows. (1) With M-2200 (the largest pore size investigated), when cooled from liquid phase, the liquid-to-D1 transition seems to be unaffected; however, the D1-to-D2 transition is shifted to lower temperatures (83°C), while the D2-to-crystal transition takes place at higher temperatures (74°C); consequently, the two transition peaks approach each other, the D1-to-D2 transition peak is broadened, while the D2-to-crystal peak is narrowed; less noticeable effects can be seen for its melting endotherms on the heating curve. (2) With the decreased pore size of M-500 and M-250, the confinement effects become more severe: the liquid-to-D1 transition temperature is slightly lowered, and the D1-to-D2 transition can no longer be observed; meanwhile, the D2-to-crystal transition peaks in the two membranes show no significant changes; upon heating, the D1 melting temperature is marginally reduced, particularly for RHO in M-250, by about 3°C.

These non-isothermal measurements are dependent on heating and cooling rates. An interesting feature in figure 2 is the supercooling of the crystallization of RHO, which is defined as the crystal melting temperature upon heating minus the crystallization temperature upon cooling. It is about 47°C for pure RHO and 38°C for confined RHO, with a cooling and heating rate of 10°C min^{-1}. We examined this property at various cooling and heating rates. It was found that pure RHO has a higher supercooling than confined RHO for most cooling rates ($\geqslant$ 5°C min^{-1}), but its supercooling decreases faster with lower cooling rates. At cooling rates $<$ 2°C min^{-1}, the supercooling actually becomes slightly larger for confined RHO. An example is given in figure 3, where the cooling curve, recorded at a rate of 1°C min^{-1}, of pure RHO is compared with that of RHO inside M-250. It is important to mention that for all cooling rates, the phase transition D1-to-D2 is present for pure RHO but absent for RHO in M-250. In other words, the absence of D2 phase in M-500 and M-250 is not related to the extent of supercooling. Therefore, these results clearly reveal confinement effects on the phase transition behaviour of RHO, including transition temperatures and the occurrence of the monotropic D2 phase.

Isothermal crystallization of RHO confined in the membranes was investigated, and the results provide more information about confinement effects. The effects were found to be more important for membranes having smaller pore sizes. In the following, the results obtained with M-250 are used as examples to illustrate changes observed in the phase transitions of RHO. Figure 4 shows the development of crystallization from the D1 phase inside M-250 for three crystallization temperatures T_c. Each DSC heating curve was recorded after holding the sample at a particular temperature for the time indicated in the figure. As with pure RHO, the global crystallization rate of confined RHO decreases with increasing crystallization temperature. The interesting new feature, however, is the double crystal melting endotherm observed at all crystallization temperatures for confined RHO. In addition to the melting peak close to 110°C, which was known for pure RHO [11], another melting peak appears at a low temperature. This melting peak becomes more prominent as the crystallization temperature is raised. These results suggest the existence of RHO crystals of two distinct structures or morphologies inside the pores. The one that melts at lower

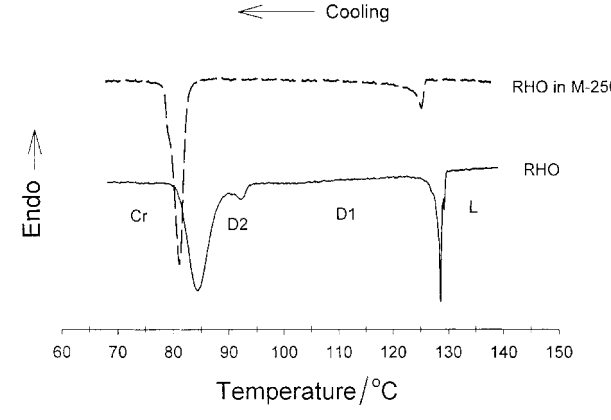

Figure 3. DSC cooling curves for RHO in the bulk and RHO in M-250, recorded at a rate of 1°C min^{-1}.

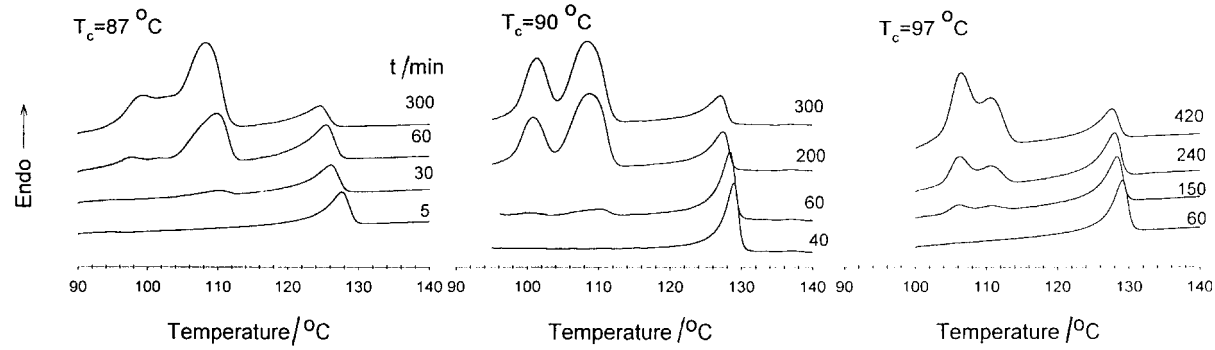

Figure 4. DSC heating curves for RHO in M-250 crystallized at three temperatures from D1 phase for the different times indicated.

temperatures is apparently formed as a result of confinement effects. It is also interesting to note that, with longer crystallization times, after the double melting of the crystal the D1 phase is affected. The D1-to-liquid transition peak is broadened and shifted to lower temperatures.

The low and high melting temperatures of RHO in M-250, $T_{m,l}$ and $T_{m,h}$, were determined for several T_c after 300 min crystallization. The results are presented in figure 5, plotting T_m as a function of T_c. Both $T_{m,l}$ and $T_{m,h}$ increase linearly as T_c increases, but the dependence of $T_{m,l}$ is greater than that of $T_{m,h}$. For comparison purpose, data for pure RHO are also shown in the figure, forming the same line as $T_{m,h}$ of RHO in M-250. It should be emphasized that for pure RHO, only one melting peak dominates with, at some crystallization temperatures, a shoulder on the melting endotherm at higher temperature (i.e., $>110°C$). Therefore, it is clear that the observed low melting temperature crystal of RHO is a result of D1-to-crystal transition inside the membrane. Moreover, the linear dependence of T_m on T_c in figure 5 can be analysed using the Gibbs–Thomson equation [12]

$$T_m = T_m^0[1 - (2\sigma/\Delta H d)] \quad (1)$$

in which T_m^0 is the equilibrium melting temperature, σ is the interfacial free energy of a mature crystallite, d is its thickness, and ΔH is the transition enthalpy per crystallizing unit.

If σ associated with a critical nucleus of thickness d^*, from which a crystallite can grow, is assumed to be the same as for a mature crystallite, the equation below is obtained [12]

$$T_m = (1 - 1/m)T_m^0 + (1/m)T_c \quad (2)$$

where $m = d/d^*$. A linear relation between T_m and T_c is expected only if m is a constant, i.e. the ratio of the thickness of a mature crystallite to the critical nucleus thickness is the same for all T_c investigated. This equation is often used to determine T_m^0 through extrapolation, since the intersection of the experimental $T_m - T_c$ plot with the line of $T_m = T_c$ should yield T_m^0. Linear regression of the data in figure 5 results in straight lines, whose intersections with the line of $T_m = T_c$ give rise to the equilibrium melting temperatures of $T_{m,l}^0 = 129°C$ ($m = 1.4$) and $T_{m,h}^0 = 114°C$ ($m = 4$). These results further imply that two types of RHO crystal are present after the D1-to-crystal transition inside the membrane.

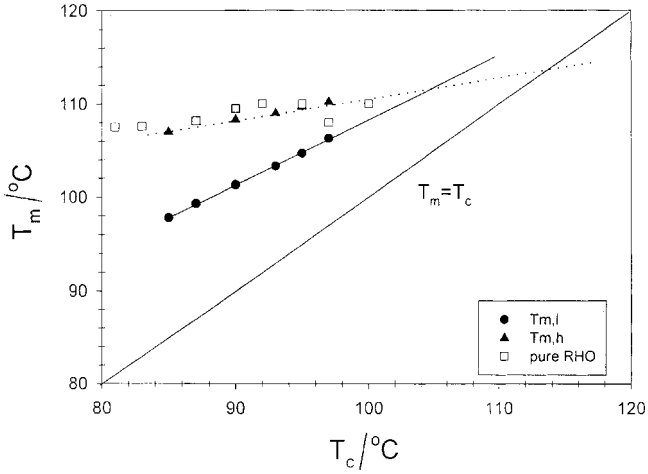

Figure 5. Double melting temperature of RHO in M-250 and the melting temperature of RHO in the bulk vs. crystallization temperature.

From the DSC curves shown in figure 4, the crystallization kinetics can be monitored by measuring the increase of the heat of fusion of crystal with time. The overlapping of the two crystal melting peaks made it difficult to measure precisely the melting heat of each peak. For this reason, the total crystal-to-D1 transition enthalpy, ΔH_c, (the sum of the two peaks) was determined and analysed. Figure 6 shows the data obtained for the three temperatures used as examples in figure 4, plotting ΔH_c vs. logarithmic crystallization time. Similar to pure RHO [11], all curves have the same shape. The difference in the global rate of crystallization is due to

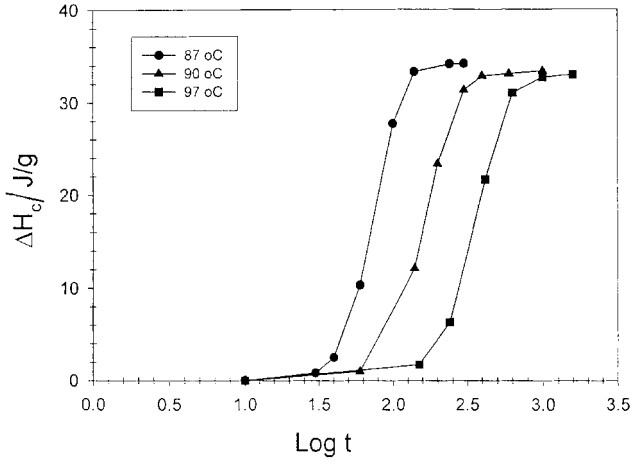

Figure 6. Melting heats of the crystal of RHO developed from the D1 phase inside M-250 vs. logarithmic crystallization time at the crystallization temperatures indicated in the figure.

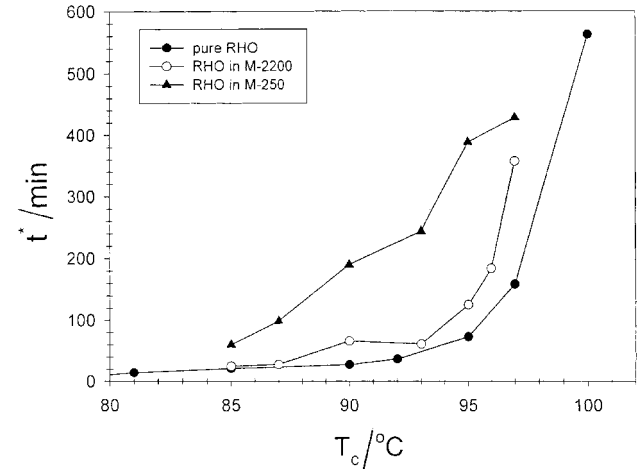

Figure 7. Characteristic time t^* for completion of 63% of crystallization vs. crystallization temperature for RHO in the bulk and RHO in M-250 and M-2200.

the induction period that is a function of temperature. The kinetics data can be analysed using the Avrami equation

$$x = 1 - \exp(-bt^n) \tag{3}$$

where x is the degree of crystallization (the volume fraction transformed from D1 to crystal) at time t; the two constants b and n depend on the nucleation mechanism and the dimensional geometry of the growing domains. From calorimetric measurements, x can be determined from $x = \Delta H_c/\Delta H_c^0$, in which ΔH_c^0 is the plateau value in figure 6. Within experimental error, ΔH_c^0 of RHO in M-250 was found to be $\sim 33\ \mathrm{J\ g^{-1}}$. Equation (3) can be changed to

$$x = 1 - \exp[-(t/t^*)^n] \tag{4}$$

where $t^* = b^{-1/n}$, which is a characteristic time that measures the global rate of crystallization, since at $t = t^*$, $x = 0.632$. The values of t^* obtained at different crystallization temperatures for RHO in M-250 and M-2200 are reported in figure 7, and compared with t^* of pure RHO. It is seen that the confinement effects on the rate of D1-to-crystal transformation are largest for membranes of small pore sizes. For most temperatures, the global rate of crystallization is only slightly slowed in M-2200 but severly reduced in M-250.

Information about the nucleation mechanism and nucleus geometry can be obtained by determining the constant n in the Avrami equation. Figure 8 shows the plot of $\log[-\ln(1 - \Delta H_c/\Delta H_c^0)]$ vs. $\log(t/t^*)$ for RHO in M-250 at five crystallization temperatures. A single straight line is formed, whose slope gives rise to $n = 2.9 \pm 0.1$. This result is similar to the $n = 3$ obtained for pure RHO [11].

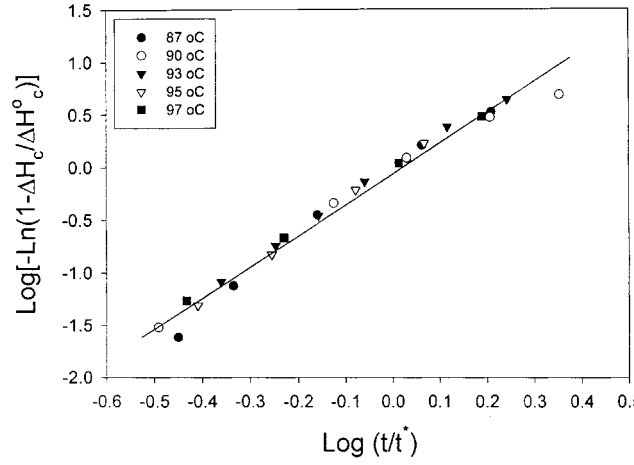

Figure 8. Avrami plots for RHO in M-250 at different crystallization temperatures. See text for details.

4. Discussion

RHO molecules have an elongated mesogenic core with a twofold rotational axis of symmetry. Assuming planar zigzag conformations for the alkyl chains, the molecular size is about 35 Å in the long axis direction of the rigid core. All Millipore membranes used have average pore sizes significantly larger than that length. This explains why discotic and crystalline phases of RHO can be formed in the randomly interconnected pores. However, when confined inside a restricted space, the phase transition behaviour of RHO is affected.

The first consequence of confinement is the suppression of the monotropic D2 phase inside the membranes of smaller pore sizes, M-500 and M-250. As can be seen from figure 2, even inside the large pore size membrane

M-2200, the transformation from D1 to D2 upon cooling is difficult to develop, with the transition shifted to lower temperatures and a diminished transition peak; no D1-to-D2 transition occurred inside M-500 and M-250. Restricted spaces inside the porous membranes should be the cause of this effect. As can be seen from the sketch in figure 1, the transition D1-to-D2 is the transformation from a columnar phase having a smaller unit cell (two columns) to another columnar phase having a larger unit cell (four columns), involving changes in the orientation of rigid cores that form the columns. This transformation takes place among columns aligned in the same direction. It is easy to picture that, inside the randomly interconnected pores, possible surface anchoring will make it difficult for many columns to align side-by-side in the same direction, particularly for small pores. Consequently, the lack of a sufficient number of columns aligned in the same direction may prevent the transformation from D1 to D2.

The second consequence of confinement is the double melting of the crystal resulting from the transformation from the D1 phase. Restricted spaces may impose changes in the crystal structures and morphology. For RHO in M-250, the maximum crystal melting heat (the sum of both peaks) ΔH_c^0 is about 33 J g^{-1} (figure 6), which is smaller than $\sim$47 J g found for pure RHO [11]. This is indicative of a loss of order of the crystalline structure of RHO inside the membrane. We do not know how RHO molecules are ordered near the wall of the pores. There are two basic possibilities [13]: the plane of the rigid core is parallel to the surface (side-on), or the plane normal is parallel to the surface (edge-on). Qualitatively, as each RHO molecule contains a rigid core and six long alkyl chains, the conformation of these flexible tails could readily be altered by the wall and by a restricted space. This could lead to a reduced order for this part of the molecules and, as a result, ordered flexible chains melting at lower temperatures. In other words, for pure RHO, the crystalline structure contains ordered rigid cores and flexible tails that melt at similar temperatures. For RHO in M-250, however, we speculate that the confinement effects could result in a decrease in order for the flexible tails in contact with the wall so that they melt before the rigid cores. The overlapping of the two melting peaks (figure 4) made it difficult to quantify the proportion of the alkyl tails affected by the wall: it was found, however, that the prominence of the low temperature melting peak decreases as the pore size increases. This is an indication that this portion of the RHO molecules is proportional to the surface-to-volume fraction of the membrane. The proposed mechanism accounting for double melting is also supported by the observed strong dependence of $T_{m,l}$ on T_c (figure 5). A similar phenomenon was observed for the crystallization of some poly(3-alkylthiophene)s [14], where the appearance of a low temperature endotherm was attributed to the crystallization of alkyl side chains, and the plot of its melting temperature vs. T_c was found to almost parallel the line of $T_m = T_c$.

Furthermore, the affected crystalline structure developed inside the membrane has some consequences on the D1 phase after melting. From the curves in figure 4, it is clear that after melting of the crystal formed from a long-time crystallization, the D1-to-liquid transition peak is broadened and lowered by about 3°C. The last significant effect due to confinement is on crystallization kinetics. For RHO in M-250, from the beginning of the D1-to-crystal transformation process, the time needed to reach 63% of crystallized volume is much longer than for pure RHO (figure 7). The difference in the global rate of crystallization is actually caused by the difference in the induction period that precedes the growth of the crystal. The observed longer induction times for effective nucleation for confined RHO may be explained by a reduced mobility of the RHO molecules inside the membrane because of restricted spaces. However, within experimental error, the same Avrami constant $n \sim 3$ was found for confined RHO and for pure RHO. This result suggests that confinement has no effect on the overall mechanism operating on the D1-to-crystal transformation. As discussed previously [11], a two-dimensional sporadic nucleation and growth characterizes the crystallization of RHO from discotic mesophases.

5. Conclusions

When discotic liquid crystal RHO is inserted into Millipore membranes that contain randomly interconnected pores, its phase transition behaviour is affected. The confinement effects hinder the transition from the enantiotropic columnar D1 phase to the monotropic columnar D2 phase, and lead to suppression of the D2 phase in membranes having average pore sizes $\leqslant$ 500 Å. The transformation from D1 to the crystalline phase is also perturbed by confinement, particularly in M-250. In this membrane, the formed crystal, on the one hand, displays a double melting endotherm, with a distinct ordered structure melting at lower temperatures. On the other hand, at a given crystallization temperature the induction period before effective crystal growth becomes much longer, resulting in a slowing of the global rate of crystallization. However, the confinement shows no effect on the overall crystallization mechanism. A similar Avrami constant of $n \sim 3$ was obtained for both confined and bulk RHO, which suggests a two-dimensional sporadic nucleation and growth. In order to elucidate the origin of the observed double melting for RHO crystallized inside the membranes, further studies using techniques such as X-ray diffraction and NMR are needed.

Financial support from the Natural Sciences and Engineering Research Council of Canada and the Fonds pour la Formation de Chercheurs et l'Aide à la Recherche of Québec is acknowledged. L. Corvazier is grateful to the Centre de Recherche en Science et Ingénierie des Macromolécules (Université Laval) for a scholarship.

References

[1] Crawford, G. P., and Zumer, S. (eds.), 1996, *Liquid Crystals in Complex Geometries Formed by Polymer and Porous Networks* (London: Taylor & Francis).
[2] Finotello, D., Iannacchione, G. S., and Qian, S., chap. 16 in ref. [1].
[3] Bellini, T., and Clark, N. A., chap. 19 in ref. [1].
[4] Rappaport, A. G., Clark, A. A., Thomas, B. N., and Bellili, T., chap. 20 in ref. [1].
[5] Aliev, F. M., chap. 17 in ref. [1].
[6] Qian, S., Iannacchione, G. S., and Finotello, D., 1997, *Mol. Cryst. liq. Cryst.*, **292,** 175.
[7] Qian, S., Iannacchione, G. S., and Finotello, D., 1996, *Phys. Rev. E*, **53,** R4291.
[8] Chandrasekhar,S., Sadashiva, B. K., and Suresh, K. A., 1977, *Pramana*, **9,** 471.
[9] Queguiner, A., Zann, A., Dubois, J. C., and Billard, J., 1980, in Proceedings of the International Conference on Liquid Crystals, edited by S. Chandrasekar (London: Heyden and Son).
[10] Billard, J., Dubois, J. C., Vaucher, C., and Levelut, A. M., 1981, *Mol. Cryst. liq. Cryst.,* **66,** 115.
[11] He, Z., Zhao, Y., and Caillè, A., 1997, *Liq. Cryst.*, **23,** 317.
[12] Alamo, R. G., Chan, E. K. M., Mandelkern, L., and Voigt-Martin, I. G., 1992, *Macromolecules*, **25,** 6381.
[13] Kruk, G., Kocot, A., Wrzalik, R., and Vij, J. K., 1993, *Liq. Cryst.*, **14,** 807.
[14] Zhao, Y., Keroack, D., Yuan, G., Massicotte, A., Hanna, R., and Leclerc, M., 1997, *Macromol. Chem. Phys.*, **198,** 1035.